A Dinuclear Nickel(II) Complex with Readily Accessible Coordination Sites and Additional N-Functional Groups in Proximity to the Bimetallic Core

Franc Meyer,* Albrecht Jacobi,† Bernhard Nuber,† Peter Rutsch,† and Laszlo Zsolnai†

Anorganisch-Chemisches Institut der Universität Heidelberg, Im Neuenheimer Feld 270, D-69120 Heidelberg, Germany

Received September 26, 1997

A series of pyrazolate-based dinuclear Ni(II) complexes relevant to the active site of urease are reported. Deprotonation of HL^1 [HL^1 = 3,5-bis(R_2NCH_2)-pyzH; $R_2N = Me_2N(CH_2)_3NMe$] by means of 1 equiv of BuLi and subsequent reaction with 2 equiv of $[Ni(H_2O)_6](ClO_4)_2$ in the presence of NEt^iPr_2 affords the dinuclear complex $[L^1Ni_2(OH)(MeCN)_2](ClO_4)_2$ (**1**). This is shown crystallographically to contain two five-coordinate nickel ions bridged by both the pyrazolate and a hydroxide, with an acetonitrile solvent molecule bound to each metal center. When HL^2 is employed {HL^2 = 3,5-bis(R_2NCH_2)-pyzH; $R_2N = [Me_2N(CH_2)_3]_2N$}, the additional ligand side arms act as proton acceptors forming an intramolecular N··H··N bridge to yield the complex $[HL^2Ni_2(OH)(MeCN)_2](ClO_4)_3$ (**2**), whose basic bimetallic framework is essentially identical to **1**. The two Ni(II) centers in **2** exhibit strong antiferromagnetic coupling ($J = -46.7$ cm^{-1}). The labile acetonitrile donors in **2** are easily replaced by either neutral ligands such as dmf or anions such as thiocyanate, giving rise to the formation of complexes $[HL^2Ni_2(OH)(dmf)_2](ClO_4)_3$ (**3**) and $[HL^2Ni_2(OH)(NCS)_2](ClO_4)$ (**4**), respectively, where the overall dinuclear framework of **2** remains unchanged upon the substitution reaction.

Introduction

Numerous enzymes that catalyze the hydrolysis of e.g. esters or amides contain more than one metal ion within their active site.[1] Among these hydrolases only urease, which degrades urea to form ammonia and carbamate, has been found to be nickel dependent.[2] An X-ray crystal structure of the microbial urease from *Klebsiella aerogenes* revealed a unique dinuclear metallobiosite with two nickel atoms 3.5 Å apart bridged by a carboxylated ϵ-amino residue of a lysin side chain.[3] On the basis of the crystallographic findings, a possible mechanism for the chemistry at the catalytic site has been suggested, where both nickel ions are involved in the hydrolysis of urea in a specific manner.[4] According to the proposed mechanism, several key features of the molecular geometry at the active site are essential for the overall function of the enzyme. These include an open coordination site at each metal center, one of which serves to bind and polarize the urea substrate that is attacked by the nucleophile, i.e., a hydroxide ion coordinated to the accessible site at the opposite nickel ion. The requisite generation of the hydroxide via removal of a proton from coordinated water is suggested to occur by the assistance of a basic histidine residue located in proximity to the bimetallic core, thus underlining the importance of additional functional groups of the surrounding protein matrix for metalloenzyme catalysis.

Several attempts to model the structure and reactivity of the urease active site have been reported,[5,6] where most of the bimetallic systems studied are composed of primary dinucleating ligands with bridging phenoxo or alkoxo groups.[6] In contrast, the chemistry of multidentate dinucleating ligands that are based on other bridging moieties is much less developed.[7] We recently described the synthesis and coordination potential of a series of pyrazolate ligands with chelating polyamino substituents in the 3- and 5-positions of the heterocycle.[8] In the present paper we present a series of dinuclear nickel(II) complexes of ligands of this type, HL^1 and HL^2 (Chart 1), where in the latter case the side-arm donors constitute part of the coordination sphere of the metal ions and at the same time provide additional basic functional groups adjacent to the dinuclear core, thereby assisting in the formation of a metal-bonded hydroxide and leaving readily accessible sites at both nickel(II) centers. Our premise is that the synthesis and study of such complexes exhibiting key features of the active center of urease could prove

* To whom correspondence should be addressed. Fax: (0049)-6221-545707. E-mail: Franc@sun0.urz.uni-heidelberg.de.

† X-ray crystallography.

(1) (a) Göbel, M. W. *Angew. Chem., Int. Ed. Engl.* **1994**, *33*, 1141. (b) Sträter, N.; Lipscomb, W. N.; Klabunde, T.; Krebs, B. *Angew. Chem., Int. Ed. Engl.* **1996**, *35*, 2024.

(2) (a) Halcrow, M. A.; Christou, G. *Chem. Rev.* **1994**, *94*, 2421. (b) Kolodziej, A. F. *Prog. Inorg. Chem.* **1994**, *41*, 493.

(3) Jabri, E.; Carr, M. B.; Hausinger, R. P.; Karplus, P. A. *Science* **1995**, *268*, 998.

(4) Lippard, S. J. *Science* **1995**, *268*, 996. See also: Dixon, N. E.; Riddles, P. W.; Gazzola, C.; Blakeley, R. L.; Zerner, B. *Can. J. Biochem.* **1980**, *58*, 1335. Karplus, P. A.; Pearson, M. A.; Hausinger, R. P. *Acc. Chem. Res.* **1997**, *30*, 330.

(5) (a) Blakeley, R. L.; Treston, A.; Andrews, R. K.; Zerner, B. *J. Am. Chem. Soc.* **1982**, *104*, 612. (b) Wages, H. E.; Taft, K. L.; Lippard, S. J. *Inorg. Chem.* **1993**, *32*, 4985.

(6) (a) Volkmer, D.; Hörstmann, A.; Griesar, K.; Haase, W.; Krebs, B. *Inorg. Chem.* **1996**, *35*, 1132. (b) Volkmer, D.; Hommerich, B.; Griesar, K.; Haase, W.; Krebs, B. *Inorg.* Chem. **1996**, *35*, 3792. (c) Yamaguchi, K.; Koshino, S.; Akagi, F.; Suzuki, M.; Uehara, A.; Suzuki, S. *J. Am. Chem. Soc.* **1997**, *119*, 5752.

(7) See for example: (a) Itoh, M.; Motoda, K.; Shindo, K.; Kamiusuki, T.; Sakiyama, H.; Matsumoto, N.; Okawa, H. *J. Chem. Soc., Dalton Trans.* **1995**, 3635. (b) Thompson, L. K.; Tandon, S. S.; Manuel, M. E. *Inorg. Chem.* **1995**, *34*, 2356. (c) Brooker, S.; Croucher, P. D.; Roxburgh, F. M. *J. Chem. Soc., Dalton Trans.* **1996**, 3031.

(8) (a) Meyer, F.; Beyreuther, S.; Heinze, K.; Zsolnai, L. *Chem. Ber./ Recueil* **1997**, *130*, 605. (b) Meyer, F.; Heinze, K.; Nuber, B.; Zsolnai, L. *J. Chem. Soc., Dalton Trans.* **1998**, 207.

S0020-1669(97)01234-2 CCC: $15.00
Published on Web 03/03/1998

Chart 1

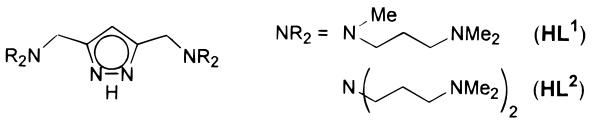

useful in elucidating the way this metalloenzyme works and at the end might lead to functional models of hydrolase enzymes.

Experimental Section

General Procedures and Methods. All manipulations were carried out under an atmosphere of dry nitrogen by employing standard Schlenk techniques. Solvents were dried according to established procedures. HL^1 and HL^2 were synthesized according to the reported method;[8a] all other chemicals were used as purchased. Microanalyses: Mikroanalytische Laboratorien des Organisch-Chemischen Instituts der Universität Heidelberg. IR spectra: Bruker IFS 66 FTIR; recorded as KBr pellets. FAB-MS spectra: Finnigan MAT 8230. UV/vis spectra: Perkin-Elmer Lambda 19. Magnetic measurement: Bruker Magnet B-E 15 C8, field-controller B-H 15, variable-temperature unit ER4111VT, Sartorius micro balance M 25 D-S. Experimental susceptibility data were corrected for the underlying diamagnetism.

Caution! *Although no problems were encountered in this work, transition metal perchlorate complexes are potentially explosive and should be handled with proper precautions.*

Synthesis of 1. HL^1 (0.21 g, 0.65 mmol) dissolved in thf (15 mL) was deprotonated by means of addition of 1 equiv of BuLi (2.5 M in hexane). After being stirred for 10 min, the solution was evaporated to dryness and the residue taken up in MeCN (25 mL) and subsequently treated with NEt^iPr_2 (0.12 mL, 0.69 mmol) and $[Ni(H_2O)_6](ClO_4)_2$ (0.48 g, 1.31 mmol). The resulting green reaction mixture was stirred at room temperature for 2 h and then reduced to a volume of ~5 mL. Addition of EtOH (35 mL) caused the precipitation of a blue-green solid, which was isolated by filtration and dried under vacuum. Layering a solution of this solid in MeCN with Et_2O afforded green crystals of **1** (0.20 g, 42%). IR (KBr, cm^{-1}): 3580 [s, ν(OH)], 2314, 2286 [s, ν(MeCN)], 1474 (s), 1081 [br, s, $\nu(ClO_4)$], 624 (s). MS (FAB+) [*m*/*z* (relative intensity)]: 639 (100), $[L^1Ni_2(OH)(MeCN)_2(ClO_4)]^+$; 557 (59), $[L^1Ni_2(OH)(ClO_4)]^+$; 455 (96), $[L^1Ni_2(OH)]^+$. Anal. Calcd for $C_{21}H_{42}Cl_2N_8Ni_2O_9$: C, 34.14; H, 5.73; N, 15.16. Found: C, 33.77; H, 5.71; N, 15.29.

Synthesis of 2. HL^2 (0.23 g, 0.49 mmol) dissolved in thf (15 mL) was deprotonated by means of addition of 1 equiv of BuLi (2.5 M in hexane). After being stirred for 10 min, the solution was evaporated to dryness and the residue taken up in MeCN (25 mL) and subsequently treated with $[Ni(H_2O)_6](ClO_4)_2$ (0.36 g, 0.98 mmol). After the resulting dark green reaction mixture was stirred at room temperature for 2 h, all volatile material was removed under vacuum. The residue was redissolved in MeCN (20 mL) and filtered. Layering the filtrate with Et_2O affords dark green crystals of **2** (0.28 g, 58%). IR (KBr, cm^{-1}): 3585 [s, ν(OH)], 2324, 2314, 2295, 2286 [m, ν(MeCN)], 1474 (s), 1076 [br, s, $\nu(ClO_4)$], 624 (s). MS (FAB+) [*m*/*z* (relative intensity)]: 781 (100), $[L^2Ni_2(OH)(MeCN)_2(ClO_4)]^+$ and $[L^2Ni_2(ClO_4)_2]^+$; 697 (59), $[L^2Ni_2(OH)(ClO_4)]^+$; 597 (30), $[L^1Ni_2(OH)]^+$. Anal. Calcd for $C_{29}H_{61}Cl_3N_{10}Ni_2O_{13}$: C, 35.48; H, 6.26; N, 14.27. Found: C, 35.40; H, 6.27; N, 14.18.

Synthesis of 3. **2** (0.30 g, 0.31 mmol) was dissolved in dmf (20 mL) and the solution layered with Et_2O. Green crystals of **3**·dmf (0.32 g, 92%) gradually formed. IR (KBr, cm^{-1}): 3413 [br, s, ν(OH)], 1649 [s, ν(C=O)], 1462 (m), 1380 (m), 1140, 1113, 1085 [s, $\nu(ClO_4)$], 625 (s). MS (FAB+) [*m*/*z* (relative intensity)]: 780 (10), $[L^2Ni_2(ClO_4)_2]^+$; 697 (25), $[L^2Ni_2(OH)(ClO_4)]^+$; 467 (100), $[HL^2]^+$. Anal. Calcd for $C_{31}H_{69}Cl_3N_8Ni_2O_{15}$: C, 36.50; H, 6.85; N, 13.77. Found: C, 36.38; H, 7.01; N, 13.74.

Synthesis of 4. **2** (0.30 g, 0.31 mmol) was dissolved in MeCN (20 mL) and NaSCN (0.05 g, 0.62 mmol) added in one portion. After being stirred at room temperature for 3 h, the reaction mixture was evaporated to dryness and the residue taken up in acetone/CH_2Cl_2 (1:1, 20 mL) and filtered. Vapor diffusion of petroleum ether (boiling range 40/60) into the solution afforded green crystalline needles of **4**·$0.3CH_2Cl_2$·H_2O (0.24 g, 86%). IR (KBr, cm^{-1}): 3442 [br, s, ν(OH)], 2077 [s, ν(NCS)], 1640 (w), 1464 (s), 1117, 1088 [br, s, $\nu(ClO_4)$], 622 (m). MS (FAB+) [*m*/*z* (relative intensity)]: 740 (30), $[L^2Ni_2(NCS)(ClO_4)]^+$; 697 (100), $[L^2Ni_2(OH)(ClO_4)]^+$; 639 (42), $[L^2Ni_2(NCS)_2]^+$. Anal. Calcd for $C_{27}H_{55}ClN_{10}Ni_2O_5S_2$·$0.3CH_2Cl_2$·$H_2O$: C, 38.12; H, 6.75; N, 16.28; S, 7.45. Found: C, 37.94; H, 6.49; N, 15.65; S, 7.00.

X-ray Crystallography. The measurements were carried out on a Siemens (Nicolet Syntex) R3m/v four-circle diffractometer with graphite-monochromated Mo Kα radiation. All calculations were performed with a micro-vax computer using the SHELXT PLUS software package. Structures were solved by direct methods with the SHELXS-86 and refined with the SHELX93 programs[9] (**1**, **2**, and **4**) or with the SHELXTL PLUS-release 4.2/800 (**3**). An absorption correction (ψ scan, $\Delta\psi = 10°$) was applied to all data. Atomic coordinates and anisotropic thermal parameters of the non-hydrogen atoms were refined by full-matrix least-squares calculation. The hydrogen atoms were placed at calculated positions and allowed to ride on the atoms they are attached to, except for the hydrogen atoms of the bridging hydroxides which could be located in the difference Fourier map and refined in all cases; the hydrogen atom of the N−H−N bridge was found and refined for **2** and could also be located for **4** but not in the case of **3**. Due to the poor quality of the crystals the structure analysis of **4** could only be refined to a final (poor) agreement value of $R = 0.102$. Table 1 compiles the data for the structure determinations.

Results and Discussion

Synthesis and General Characterization. With the aim of preparing a dinuclear nickel(II) complex that possesses vacant coordination sites suitable for the binding of potential substrate molecules, we first chose the pyrazolate ligand L^1 which provides fewer donor sites than required to coordinately saturate a nickel(II) ion within each coordination compartment. Deprotonation of HL^1 by means of BuLi and subsequent addition of 2 equiv of $[Ni(H_2O)_6](ClO_4)_2$ in the presence of acetonitrile immediately yields a dark green solution, from which dark green crystals of $[L^1Ni_2(OH)(MeCN)_2](ClO_4)_2$ (**1**) can be isolated. The UV/vis spectral features of **1** (Table 2) bear close resemblance to band positions reported for trigonal bipyramidal high-spin nickel(II) compounds,[10] thus suggesting five-coordination of the metal centers in solution. This also proves true in the solid state as revealed by an X-ray crystal structure analysis. **1** crystallizes in the monoclinic space group $P2_1/n$ with four molecular entities in the unit cell. Selected atom distances and bond angles are given in Table 3; the structure of the cation is depicted in Figure 1. It contains a dinuclear nickel core in which both metal ions are spanned by the pyrazolate and a hydroxide. The proton of the bridging hydroxide forms a weak hydrogen bridge to a perchlorate counteranion [d(O1···O2) = 3.204 Å]. The metal−metal distance amounts to 3.493 Å with the coordination geometry around each nickel atom being intermediate between TB-5 and SPY-5. Each two of the N donor atoms within the substituents of the heterocycle are bonded to the nickel ions, thus leaving vacant coordination sites at both metal centers which are occupied by acetonitrile solvent molecules. The presence of the latter as well as the presence of the hydroxide group is further corroborated by the occurrence of sharp IR absorptions at 2286, 2314, and 3585 cm^{-1}, respectively.

It is reasonable to assume that the metal-bonded hydroxide originates from a water molecule of the starting material, and

(9) Sheldrick, G. M. *SHELX 93, Program for Crystal Structure Refinement*; Universität Göttingen: Göttingen, Germany, 1993. Sheldrick, G. M. *SHELXS 86, Program for Crystal Structure Solution*; Universität Göttingen: Göttingen, Germany, 1986.

(10) (a) Ciampolini, M.; Nardi, N.; Speroni, G. P. *Coord. Chem. Rev.* **1966**, *1*, 222. (b) Furlani, C. *Coord. Chem. Rev.* **1968**, *3*, 141.

Table 1. Crystal Data and Refinement Details for Complexes **1**−**4**

	1	**2**	**3**	**4**
formula	$C_{21}H_{42}Cl_2N_8Ni_2O_9$	$C_{29}H_{61}Cl_3N_{10}Ni_2O_{13}$	$C_{31}H_{69}Cl_3N_{10}Ni_2O_{15}\cdot C_3H_7NO$	$C_{27}H_{55}ClN_{10}Ni_2O_5S_2\cdot 0.3CH_2Cl_2\cdot H_2O$
M_r	738.9	981.6	1118.8	863.0
cryst size (mm)	0.20 × 0.15 × 0.25	0.30 × 0.30 × 0.20	0.40 × 0.90 × 1.10	0.20 × 0.30 × 0.40
cryst system	monoclinic	monoclinic	monoclinic	tetragonal
space group	$P2_1/n$	$P2_1$	$P2_1/n$	$P4_2/n$
a (Å)	13.218(5)	12.370(2)	12.544(4)	30.337(6)
b (Å)	15.284(6)	18.444(4)	13.831(5)	30.337(6)
c (Å)	17.201(7)	19.352(4)	30.25(1)	9.493(2)
β (deg)	109.43(3)	95.63(1)	95.26(3)	90
V (Å^3)	3277(2)	4394(2)	5226(3)	8737(3)
ρ_{calcd} (g cm^{-3})	1.498	1.475	1.42	1.309
Z	4	4	4	8
F(000) (e)	1544	2040	2368	3632
T (K)	200	200	295	200
μ(Mo $K\alpha$) (mm^{-1})	1.369	1.107	0.95	1.106
scan mode	ω	ω	ω	ω
hkl range	−7 to 15, −8 to 18, ±20	−3 to 14, −18 to 21, ±22	±16, 0−18, 0−38	−14 to 31, −15 to 34, ±10
2θ range (deg)	3.7−50.0	3.2−48.0	3.0−52.0	2.7−47.0
measd reflcns	5650	8524	10 106	6523
obsd reflcns	2227 [$I > 2\sigma(I)$]	4517 [$I > 2\sigma(I)$]	6019 [$I > 2.5\sigma(I)$]	3125 [$I > 2\sigma(I)$]
refined params	394	529	596	453
resid electron dens (e Å^{-3})	0.814/−0.564	0.977/−0.612	0.93/−0.89	1.29/−0.80
R	0.082	0.058	0.076	0.102
wR	0.199 (F^2, all data)	0.147 (F^2, all data)	0.065 (F, obsd data)	0.322 (F^2, all data)

Table 2. UV/Vis Data for the Complexes ($\tilde{\nu}$ in nm, ϵ in M^{-1} cm^{-1})

1	385 (290), 460 (55), 610 (105)
2	389 (320), 458 (72), 616 (111)
3	398(180), 460 (39, sh), 648 (60)
4	401 (300), 466 (67, sh), 647 (94)

Table 3. Selected Atom Distances (Å) and Angles (deg) for **1**

Ni1−N1	1.975(9)	Ni2−O1	1.990(8)
Ni1−O1	1.972(8)	Ni2−N3	2.171(9)
Ni1−N6	2.187(9)	Ni2−N4	2.047(9)
Ni1−N7	2.04(1)	Ni2−N5	2.05(1)
Ni1−N8	2.05(1)	N1−N2	1.34(1)
Ni2−N2	1.98(1)	Ni1···Ni2	3.493
N1−Ni1−O1	85.2(4)	N2−Ni2−N4	105.3(4)
N1−Ni1−N6	78.8(4)	N2−Ni2−N5	159.3(4)
N1−Ni1−N7	106.9(4)	O1−Ni2−N3	150.4(3)
N1−Ni1−N8	159.0(4)	O1−Ni2−N4	111.2(4)
O1−Ni1−N6	151.5(3)	O1−Ni2−N5	92.7(4)
O1−Ni1−N7	108.8(4)	N3−Ni2−N4	97.1(4)
O1−Ni1−N8	91.2(4)	N3−Ni2−N5	93.5(4)
N6−Ni1−N7	98.4(4)	N4−Ni2−N5	94.8(4)
N6−Ni1−N8	95.4(4)	Ni1−N1−N2	122.9(7)
N7−Ni1−N8	93.9(4)	Ni2−N2−N1	122.8(7)
N2−Ni2−O1	84.7(4)	Ni1−O1−Ni2	123.7(4)
N2−Ni2−N3	79.5(4)		

consequently, the yield of **1** is significantly improved by the addition of 1 equiv of a base like ethyldiisopropylamine acting as the acceptor for the liberated proton. When a similar synthetic procedure without addition of an external base is performed starting from the ligand HL[2] (which contains appended side arms possessing basic amine nitrogen atoms) complex **2** is obtained, whose spectral characteristics are very similar to those of **1** (Table 2), in particular showing IR absorptions in the range expected for coordinated acetonitrile and a sharp band at 3585 cm^{-1} assigned to the ν(O−H) stretching vibration. The result of an X-ray crystallographic analysis of **2** is depicted in Figure 2.

It reveals a dinuclear structure that is essentially identical to the basic bimetallic core of **1**, i.e., consisting of two nickel centers 3.476 Å apart spanned by both the pyrazolate of the primary ligand and a hydroxide. Selected atom distances and bond angles are listed in Table 4. The remaining additional

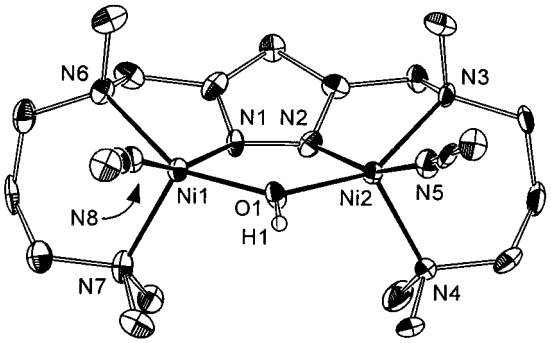

Figure 1. View of the molecular structure of the cation of **1** (30% probability ellipsoids). In the interests of clarity the hydrogen atoms except H1 have been omitted.

side arms in **2** are dangling (noncoordinating) and clutch a proton located as a strong hydrogen bridge between N5 and N8 [d(N5···N8) = 2.751 Å]. As in the case of **1**, the proton of the hydroxide spanning the two nickel centers forms a weak hydrogen bridge to one of the perchlorate counteranions [d(O1···O4) = 3.124 Å]. While the bridging hydroxide is evident from the IR spectrum (vide supra), the presence of both an OH group and a N−H−N bridge simply follows from counting the electrostatic charges. Presumably the proton generated by the dissociation of the water molecule that eventually forms the metal-bonded hydroxide bridge is picked up by the nearby basic side arm amine donors in **2**. Thus **2** reflects several of the key features proposed to be essential for the catalytic activity of the active site of urease, namely two nickel(II) centers at a distance of around 3.5 Å with accessible coordination sites and a metal-bonded hydroxide that is generated from coordinated water by the assistance of neighboring basic amine functions.[4]

Magnetic Properties of 2. The magnetic properties of **2** in the solid state have been studied at 1.0 T, over the temperature range 10−290 K. The data obtained for the molar susceptibility and the effective magnetic moment are plotted in Figure 3. The magnetic moment per nickel ion gradually decreases from 3.84 μ_B at 290 K to 0.98 μ_B at 10 K, while the susceptibility curve exhibits a broad maximum at around 120 K, this behavior being

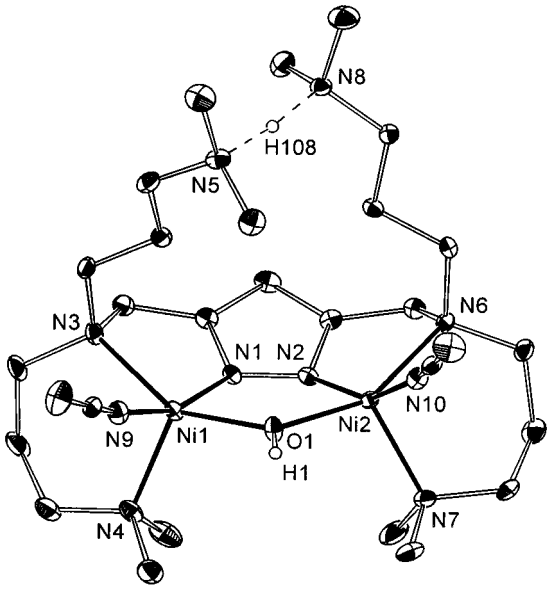

Figure 2. View of the molecular structure of the cation of **2** (30% probability ellipsoids). In the interests of clarity the hydrogen atoms except H1 and H108 have been omitted.

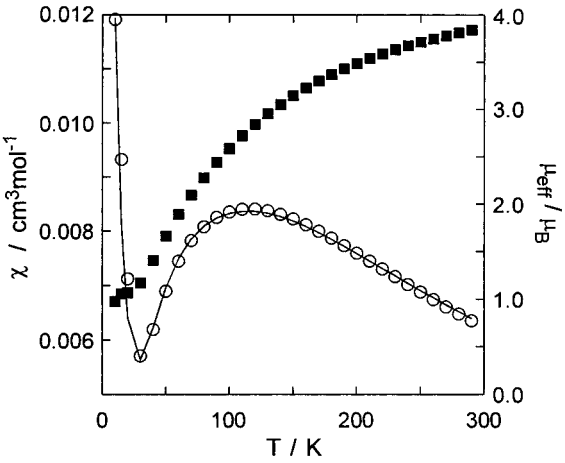

Figure 3. Temperature dependence of the molar magnetic susceptibility (open circles) and magnetic moment (solid squares) per nickel atom for **2**.

Table 4. Selected Atom Distances (Å) and Angles (deg) for **2**

Ni1−N1	1.965(4)	Ni2−N6	2.194(5)
Ni1−O1	1.980(4)	Ni2−N7	2.052(5)
Ni1−N3	2.167(5)	Ni2−N10	2.016(5)
Ni1−N4	2.060(5)	N1−N2	1.356(6)
Ni1−N9	2.051(5)	Ni1···Ni2	3.476
Ni2−N2	1.972(4)	N5···N8	2.751
Ni2−O1	1.969(4)		
N1−Ni1−O1	84.9(2)	N2−Ni2−N7	106.5(2)
N1−Ni1−N3	79.3(2)	N2−Ni2−N10	155.4(2)
N1−Ni1−N4	102.3(2)	O1−Ni2−N6	154.5(2)
N1−Ni1−N9	161.4(2)	O1−Ni2−N7	106.1(2)
O1−Ni1−N3	149.6(2)	O1−Ni2−N10	92.1(2)
O1−Ni1−N4	109.2(2)	N6−Ni2−N7	98.1(2)
O1−Ni1−N9	93.9(2)	N6−Ni2−N10	92.6(2)
N3−Ni1−N4	99.4(2)	N7−Ni2−N10	97.7(2)
N3−Ni1−N9	93.0(2)	Ni1−N1−N2	123.9(3)
N4−Ni1−N9	95.7(2)	Ni2−N2−N1	120.8(3)
N2−Ni2−O1	85.8(2)	Ni1−O1−Ni2	123.4(2)
N2−Ni2−N6	79.6(2)		

indicative of antiferromagnetic coupling between the two nickel(II) centers. An increase of the susceptibility values at very low temperatures is probably due to the presence of small amounts of uncoupled paramagnetic impurity. Fitting the experimental data to the theoretical expression for the isotropic spin-Hamiltonian $\boldsymbol{H} = -2J\cdot\boldsymbol{S}_1\cdot\boldsymbol{S}_2$ (with $S_1 = S_2 = 1$) including a molar fraction p of uncoupled paramagnetic impurity (eq 1)[11,12]

$$\chi = \chi_{\mathrm{dim}}(1 - p) + 2\chi_{\mathrm{mono}}\, p + 2N_\alpha$$

yields $J = -46.7$ cm^{-1}, $g = 2.31$, and $p = 4.6\%$. In principle powder measurements are not ideally suited for a thorough analysis of $S = 1$ dinuclear systems; however the intradimer exchange term J often proved to be the dominant term in the spin Hamiltonian[6,13] and accordingly the neglect of both a zero-field splitting parameter D and interdimer interactions $z'J'$ results in a good quality fit in the present case (Figure 3). The value of $J = -46.7$ cm^{-1} in **2** lies in the upper range of the exchange interactions reported previously for OH- or pyrazolate-bridged nickel(II) dimers.[13,14] We assume that the dominant pathway for magnetic exchange in **2** is propagated via the hydroxide bridge, although a significant contribution from the bridging pyrazolate cannot be ruled out.[14] Magneto−structural relationships for dinuclear Ni(II) systems are not yet as elaborated as the detailed correlations noted in Cu(II)/Cu(II) chemistry.[15] Only recently a linear dependence of the antiferromagnetic exchange coupling constant on Ni−O−Ni bridge angles as well as on the intramolecular Ni···Ni distance in a series of doubly phenoxy-bridged dinickel(II) complexes emerged.[16] From those studies it was concluded that the antiferromagnetic exchange interaction increases with an increase of the bridge angle Ni−O−Ni involved in the superexchange pathway and that it gets substantially augmented when going from six-coordinate species to five-coordinate square pyramidal species. Our observation of a rather large coupling constant for the five-coordinate nickel(II) centers in **2** showing a large Ni−O−Ni angle of 123.4(2)° at the bridging OH group is thus in good agreement with the reported trend.

Reactivity of 2. The ability to coordinate potential substrates to accessible coordination sites at the metal centers is an important aspect of achieving cooperative reactivity at dinuclear systems. The possible replacement of the weakly bound acetonitrile solvent molecules in **2** by either neutral or anionic ligands is demonstrated by dissolving **2** in dmf or by reacting it with 2 equiv of sodium thiocyanate, yielding the green complexes $[HL^2Ni_2(OH)(dmf)_2](ClO_4)_3$ (**3**) and $[HL^2Ni_2(OH)(NCS)_2](ClO_4)$ (**4**), respectively (Scheme 1). The incorporation of dmf in **3** is evident from the MS and IR spectra, the latter showing a broad intense band at 1649 cm^{-1} attributed to the ν(C═O) vibration of coordinated dmf and revealing the absence of any absorption in the range typical for coordinated acetonitrile. Final confirmation comes from an X-ray crystallographic analysis on single crystals that formed when the solution obtained by dissolving **2** in dmf was layered with Et_2O. The

(11) O'Connor, C. J. *Prog. Inorg. Chem.* **1982**, *29*, 203.
(12) N_α refers to the temperature-independent paramagnetism [100×10^{-6} cm^3/mol per nickel(II) ion[15b]; all other parameters have their usual meaning. $\chi_{\mathrm{dim}} = (Ng^2\mu_B{}^2/kT)[2\exp(2J/kT) + 10\exp(6J/kT)]/[1 + 3\exp(2J/kT) + 5\exp(6J/kT)]$. $\chi_{\mathrm{mono}} = 2Ng^2\mu_B{}^2/3kT$.
(13) Chauduri, P.; Küppers, H.-J.; Wieghardt, K.; Gehring, S.; Haase, W.; Nuber, B.; Weiss, J. *J. Chem. Soc., Dalton Trans.* **1988**, 1367.
(14) Fabretti, A. C.; Malavasi, W.; Gatteschi, D.; Sessoli, R. *J. Chem. Soc., Dalton Trans.* **1991**, 2331.
(15) (a) Crawford, V. M.; Richardson, M. W.; Wasson, J. R.; Hodgson, D. J.; Hatfield, W. E. *Inorg. Chem.* **1976**, *15*, 2107. (b) Kahn, O. *Molecular Magnetism*; VCH: Weinheim, Germany, 1993.
(16) (a) Nanda, K. K.; Das, R.; Thompson, L. K.; Venkatsubramanian, K.; Paul, P.; Nag, K. *Inorg. Chem.* **1994**, *33*, 1188. (b) Nanda, K. K.; Thompson, L. K.; Bridson, J. N.; Nag, K. *J. Chem. Soc., Chem. Commun.* **1994**, 1337.

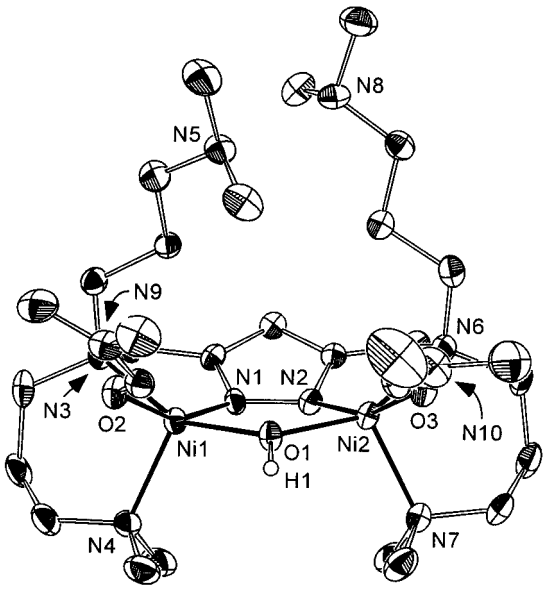

Figure 4. View of the molecular structure of the cation of **3** (30% probability ellipsoids). In the interests of clarity the hydrogen atoms except H1 have been omitted.

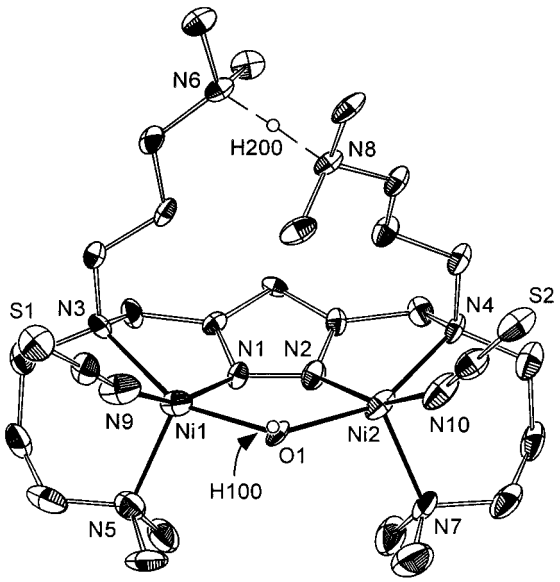

Figure 5. View of the molecular structure of the cation of **4** (30% probability ellipsoids). In the interests of clarity the hydrogen atoms except H100 and H200 have been omitted.

Scheme 1

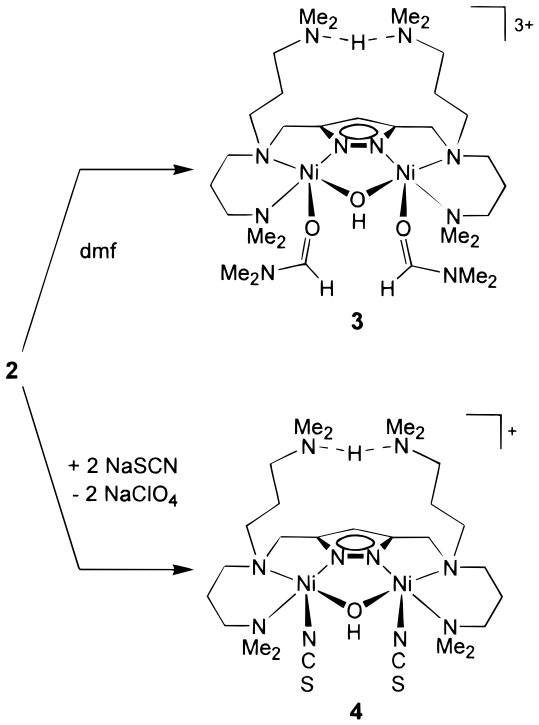

structure of the complex is depicted in Figure 4; selected atom distances and bond angles are given in Table 5.

Compound **3** crystallizes in the monoclinic space group $P2_1/n$ with one additional dmf solvent molecule per formula unit. The molecular structure reveals that the basic structural motif observed in **2** remains unchanged during the substitution reaction to form **3**; solely the labile acetonitrile ligands have been displaced by two O-bound dmf molecules. The Ni···Ni distance turns out to be slightly elongated (3.501 Å in **3** vs 3.476 Å in **2**). The proton of the bridging hydroxide is again found to form a weak hydrogen bridge to one of the perchlorate counteranions [d(O1···O11) = 3.078 Å]. Although the hydrogen atom of the N−H−N bridge could not be located in the crystallographic analysis of **3**, its presence simply follows from counting the

Table 5. Selected Atom Distances (Å) and Angles (deg) for **3**

Ni1−N1	1.949(6)	Ni2−N6	2.199(6)
Ni1−O1	2.010(5)	Ni2−N7	2.067(6)
Ni1−N3	2.194(6)	Ni2−O3	2.024(6)
Ni1−N4	2.056(7)	N1−N2	1.365(8)
Ni1−O2	2.058(5)	Ni1···Ni2	3.501
Ni2−N2	1.942(6)	N5···N8	2.779
Ni2−O1	2.025(4)		
N1−Ni1−O1	86.3(2)	N2−Ni2−N7	105.4(2)
N1−Ni1−N3	78.5(2)	N2−Ni2−O3	158.7(2)
N1−Ni1−N4	106.8(2)	O1−Ni2−N6	153.9(2)
N1−Ni1−O2	155.2(2)	O1−Ni2−N7	106.0(2)
O1−Ni1−N3	152.8(2)	O1−Ni2−O3	95.6(2)
O1−Ni1−N4	107.8(2)	N6−Ni2−N7	98.6(2)
O1−Ni1−O2	95.6(2)	N6−Ni2−O3	90.9(2)
N3−Ni1−N4	98.2(2)	N7−Ni2−O3	94.6(2)
N3−Ni1−O2	89.2(2)	Ni1−N1−N2	123.3(3)
N4−Ni1−O2	96.1(2)	Ni2−N2−N1	123.3(3)
N2−Ni2−O1	86.2(2)	Ni1−O1−Ni2	120.4(2)
N2−Ni2−N6	78.9(2)		

electrostatic charges and is further corroborated by the short distance of the corresponding nitrogen atoms [d(N5···N8) = 2.779 Å] and the close similarity between **2** and **3**.

Analogous to the case of **3**, the incorporation of thiocyanate in **4** is suggested by the MS and IR spectra, the latter showing a broad intense band at 2077 cm^{-1} assigned to coordinated thiocyanate and revealing the absence of any absorption in the range typical for coordinated acetonitrile. An X-ray crystallographic analysis on single crystals obtained from vapor diffusion of petroleum ether into a solution of **4** in acetone/CH_2Cl_2 (1:1; containing traces of water) confirmed the proposed structure, which stems from a substitution of the acetonitrile molecules in **2** by N-bound thiocyanate ligands with preservation of the overall dinuclear framework. The structure of the complex is depicted in Figure 5; selected atom distances and bond angles are given in Table 6.

The close similarity of the N···H···N distances of the dangling side arms in **2**−**4** (**2**, 2.751 Å; **3**, 2.779 Å; **4**, 2.758 Å) corroborates the presence of the hydrogen bridge in each case. A structural comparison of the basic dinuclear skeleton in **1**−**4** reveals that the atom distances from the nickel ions to the nitrogen donor atoms of L^1 and L^2 are largely uninfluenced by

Table 6. Selected Atom Distances (Å) and Angles (deg) for **4**

Ni1−N1	1.97(1)	Ni2−N10	2.03(1)
Ni1−O1	2.153(8)	N1−N2	1.35(1)
Ni1−N3	2.22(1)	N9−C26	1.18(2)
Ni1−N5	2.07(1)	C26−S1	1.60(2)
Ni1−N9	1.99(1)	N10−C27	1.15(2)
Ni2−N2	1.98(1)	C27−S2	1.64(2)
Ni2−O1	2.189(8)	Ni1···Ni2	3.638
Ni2−N4	2.20(0)	N5···N8	2.758
Ni2−N7	2.04(1)		
N1−Ni1−O1	88.5(4)	N2−Ni2−N7	105.6(5)
N1−Ni1−N3	78.6(4)	N2−Ni2−N10	157.3(5)
N1−Ni1−N5	104.1(5)	O1−Ni2−N4	154.7(3)
N1−Ni1−N9	157.9(5)	O1−Ni2−N7	104.6(5)
O1−Ni1−N3	155.2(4)	O1−Ni2−N10	93.3(5)
O1−Ni1−N5	104.3(4)	N4−Ni2−N7	99.5(5)
O1−Ni1−N9	92.8(5)	N4−Ni2−N10	91.7(5)
N3−Ni1−N5	99.4(5)	N7−Ni2−N10	96.5(5)
N3−Ni1−N9	91.6(5)	Ni1−N1−N2	124.0(8)
N5−Ni1−N9	97.1(5)	Ni2−N2−N1	126.7(8)
N2−Ni2−O1	86.5(4)	Ni1−O1−Ni2	113.8(4)
N2−Ni2−N4	79.6(4)		

the variation of the exchangeable terminal ligands. However, a considerable increase of the Ni···Ni separation is observed upon exchange of the acetonitrile ligand in **2** for dmf or in particular for thiocyanate [d(Ni···Ni) = 3.493 (**1**), 3.476 (**2**), 3.501 (**3**), 3.638 Å (**4**)], this trend being associated with a significant lengthening of the Ni−O_{bridge} bonds [d(Ni−O) = 1.972(8)/1.990(8) (**1**), 1.969(4)/1.980(4) (**2**), 2.010(5)/2.025(4) (**3**), 2.153(8)/2.189(8) Å (**4**)] and a corresponding decrease of the Ni−O−Ni bridging angle [∠(Ni−O−Ni) = 123.7(4) (**1**), 123.4(2) (**2**), 120.4(2) (**3**), 113.8(4)° (**4**)].

Unfortunately, attempts to coordinate urea to the nickel centers of the dinuclear complexes investigated in this work hitherto failed, and none of the compounds showed hydrolytic activity toward urea. One likely reason for the lack of hydrolytic activity of **2** is the tight fixation of the nickel-bound hydroxide in a bridging position, which counteracts its requisite nucleophilic character toward substrate molecules. In contrast, the ethanolysis of urea is catalyzed by some dinuclear Ni(II) complexes reported recently.[6c] In these systems a dinucleating alkoxide ligand and a bidentate secondary acetate or hydrogen carbonate bridge provide a total of 10 donor atoms, while a sixth coordination site at each Ni(II) center is available for solvent or substrate binding. This latter arrangement of two hexacoordinate Ni(II) ions with cis-oriented active coordination sites obviously allows a sterically more suitable position for the reactants (urea and ethanol), while the secondary bridge prevents a possibly deactivating bridging position of the nucleophile.

Conclusions

Novel dinuclear Ni(II) complexes based on multidentate pyrazolate-based ligands have been synthesized, which mimic some of the basic characteristics of the active site of urease. In particular, compound **2** shows two nickel ions at a distance of slightly less than 3.5 Å, intramolecular basic amine functions acting as proton abstractors to generate a metal-bound hydroxide from water, and readily accessible coordination sites occupied by labile acetonitrile solvent molecules at each metal center. The acetonitrile ligands are easily replaced by either neutral donors such as dmf or anionic moieties such as thiocyanate to yield complexes **3** and **4**, respectively, where the substitution occurs under preservation of the overall bimetallic framework and the intramolecular N−H−N bond found for **2**. Compound **2** exhibits strong antiferromagnetic coupling between the two nickel(II) centers which is rationalized on the basis of the magnetic behavior of previously reported dinickel complexes, i.e., by the structurally observed large Ni−O−Ni angle and the five-coordination of the metal centers. Unfortunately, all complexes investigated in this study lack hydrolytic activity toward urea, one reason for this presumably being the tight fixation of the nickel-bound hydroxide in a bridging position spanning the two metal centers. Attempts to increase the metal−metal separation by varying the ligand side arms and thus activate the nucleophilic hydroxide are currently underway.

Acknowledgment. We are grateful to Prof. Dr. G. Huttner for his generous support and continuous interest in our work as well as to the Deutsche Forschungsgemeinschaft (Habilitandenstipendium for F.M.) and the Fonds der Chemischen Industrie for financial support. Dr. C. Krebs and Prof. Dr. K. Wieghardt are sincerely thanked for collecting magnetic susceptibility data for **2**.

Supporting Information Available: Listings of crystallographic data, positional and thermal parameters, and interatomic distances and angles for **1**−**4** (32 pages). Ordering information is given on any current masthead page.

IC971234V